Desalination and Water Treatment
www.deswater.com
doi: 10.1080/19443994.2015.1074121

57 (2016) 15848–15861
July

Taylor & Francis
Taylor & Francis Group

Adsorption of methylene blue on chemically modified pine nut shells in single and binary systems: isotherms, kinetics, and thermodynamic studies

Mu Naushad[a], Moonis Ali Khan[a,*], Zeid Abdullah Alothman[a], Mohammad Rizwan Khan[a], Mahendra Kumar[b]

[a]*Advanced Materials Research Chair, Department of Chemistry, College of Science, Bld#5, King Saud University, P.O. Box 2455, Riyadh 11451, Saudi Arabia, Tel. +966 14674198; Fax: +966 14675992; emails: mnaushad@ksu.edu.sa (M. Naushad), mokhan@ksu.edu.sa (M. Ali Khan), zaothman@ksu.edu.sa (Z. Abdullah Alothman), mrkhan@ksu.edu.sa (M. Rizwan Khan)*
[b]*School of Biotechnology, Dublin City University, Dublin 9, Ireland, email: mahendracsmcri@gmail.com*

Received 27 January 2015; Accepted 13 July 2015

ABSTRACT

In the present work, modified sodium hydroxide-treated pine nut shells (PNSM) were used for the selective removal of methylene blue (MB) from the single and binary (with amaranth dye) systems by batch method. The material was characterized and identified by different techniques such as X-ray diffraction, Brunauer, Emmett and Teller, Fourier transform infrared and scanning electron microscopy (SEM). The distinctive properties such as low pore volume (0.060 cc/g), high surface area (>266 m^2/g), and existence of a variety of functional groups made it feasible for the removal of MB efficiently. Maximum MB adsorption (39.73 mg/g) was observed at pH_i 5.9. In the binary component system, the amaranth dye played a significant role to enhance the MB adsorption. Kinetic modeling studies showed the applicability of a pseudo-second-order model for the selective adsorption of MB in single and binary systems. Thermodynamic factors suggested that the adsorption was chemical, spontaneous, and endothermic in nature. Desorption studies showed optimum MB recovery (92.54%) with 0.1 M oxalic acid solution. The outcomes revealed that the used agricultural waste was a probable cost-effective adsorbent for the selective removal of MB from aqueous medium.

Keywords: Pine nut shells; Selective adsorption; Methylene blue; Amaranth; Desorption

1. Introduction

Large quantities of toxic dyes and pigments are generated from dye manufacturing, textile, rubber, paper, leather, plastic, cosmetic, and printing industries. These dyes and pigments as waste effluents are discharged in water resources, directly or indirectly posing severe health hazards to living beings [1]. Every year more than 10,000 dyes with 7×10^5 metric tons production are commercially available. Five to ten percentage of these dyes are lost as industrial waste effluents [2]. The occurrence of dyes in aquatic systems decreases light diffusion which slows down the photosynthetic activity and also exhibits the capability to chelate metal ions generating microtoxicity to fish and other organisms [3]. The acid dyes and water-soluble reactive removal are very severe because they tend to pass through the traditional treatment

*Corresponding author.

procedures. Thus, for the removal of such dyes from aqueous mediums, efficient treatment procedures are required. A variety of chemical, physical, and biological treatment procedures, including coagulation, adsorption, solvent extraction, membrane filtration, precipitation, chemical oxidation, and bioaccumulation have been extensively used for the treatment of dye-bearing wastewater [4]. Among these techniques, adsorption process is noted to be superior because it is economical, efficient, and simple [5–10]. Activated carbon is known to be the most extensively employed adsorbent for the removal of dyes because of its high-adsorption capacity and effectiveness; nevertheless, its utilization is still limited owing to high operational costs [11]. Therefore, there is a growing interest to search for alternative materials, which are inexpensive and locally obtainable so that the adsorption procedure will become inexpensively viable. Numerous non-conventional, low-cost adsorbents such as saw dust [12], fly ash [13], wheat straw [14], fungus [15], orange peels [16], and soy meal hull [17] have been efficiently used for the removal of various types of dyes from wastewater. The utilization of agricultural waste as adsorbent for the abatement of dyes has drawn awareness of many researchers as it is richly available, ecologically safe; there is no need to regenerate these adsorbents (unlike activated carbon, where regeneration is necessary); the majority of the types of agricultural waste do not require a complex pretreatment step or activation process before applications; and less maintenance and supervision are required for the process operation [11]. Scientists have also used various types of adsorbents for the removal of dyes from single and binary systems [18–20].

Every year, large quantities of pine nut shells (PNS) (family *Pinaceae*, genus *Pinus*) are produced as agricultural by-products all over the world. To the best of our knowledge, no one used PNS for dye removal. Most of the previous studies targeted the application of agricultural by-products for dye removal in a single system [21–24]. Industrial discharges usually contain mixtures of dyes along with other organic and inorganic matrices [25,26] and inadequate data are available on multi-component dye adsorption. Therefore, considering the formulation of industrial effluents in this work, we modified PNS by treating them with sodium hydroxide. The modified PNS were termed as PNSM and thereafter, studied the adsorption of methylene blue (MB) dye in single and binary (with amaranth dye) systems on PNSM. The effect of matrix on MB adsorption was tested by taking various counter ions to aqueous phase. The commercial feasibility of the process was established by desorption studies.

2. Experimental

2.1. Chemicals and reagents

The MB (chemical formula: $C_{16}H_{18}N_3OS$; formula mass: 333.6 g/mol; λmax: 670 nm) and amaranth dye (chemical formula: $C_{20}H_{11}N_2Na_3S_3$; formula mass: 604.47 g/mol; λmax: 520 nm) were supplied by Merck, Germany. Sodium hydroxide and HCl were purchased by BDH Laboratory Supplies Poole, England. The stock solutions of both dyes (500 mg/L) were prepared in Milli-Q water and used for further dilutions. Water was purified through a Milli-Q water purification system (Millipore Corporation, Bedford, MA, USA). Other chemicals and reagents used were of analytical reagent grade or as specified.

2.2. Preparation of PNS adsorbent

The PNS were collected from the local supermarket, Riyadh, Saudi Arabia. To eliminate the adhering dirt and soluble impurities, the PNS was first washed with distilled water and then dried at 60°C for 24 h. The dried PNS biomass was ground in a mortar and sieved to 0.2–0.4-mm particle size. The existing organic content of the PNS was oxidized by treating 1.0 g of PNS with 100 mL hydrogen peroxide (30% w/w) and the consequential mixture was kept on magnetic stirrer for 60 min at 50°C and 100 rpm. To remove the traces of hydrogen peroxide, the washing of PNS biomass was done several times with distilled water. The oxidized biomass was again treated with 0.1 M NaOH with a water bath shaker at 25°C for 24 h with constant stirring at 100 rpm. The chemically modified PNS (PNSM) was washed with distilled water to get neutral pH. The consequential PNSM biomass was dried in an oven at 65°C for 24 h to get constant weight.

2.3. Characterization of PNS biomass

The surface properties of unmodified and chemically PNSM were studied by N_2 adsorption–desorption isotherm at 77 K (Sorptomatic V 1.03). To determine functional groups present on biomass before and after modification and involved in MB adsorption Fourier transform infrared (FTIR) (Nicolet 6700 FTIR Thermo Scientific) analysis was performed. The morphology of surface for biomass was studied by scanning electronic microscopy (SEM) (SEM, Hitachi Co., Japan, Model No. S3400N). To determine the point of zero charge (pH_{PZC}) of PNSM biomass, the solid addition method [27] was used. The surface active (acid and basic) sites present on PNSM were determined by Boehm's acid–base titration experiments [28].

2.4. Adsorption studies

The adsorption of dyes onto PNSM was studied by the batch method. The adsorption experiments were made in 250 mL glass conical flasks. For the single component system, 0.4-g PNSM were added to 40 mL of MB dye solution of known concentration. The solution was continuously stirred at 100 rpm at ambient temperature (298 K) conditions for 24 h to achieve the equilibration time. The initial pH of adsorbate solution was adjusted by adding required amounts of 0.1 M HNO_3/NaOH solutions. At equilibration, PNSM was filtered off and the concentrations of MB dye in the solution phase before and after adsorption were determined using a double beam UV–vis spectrophotometer. A number of parameters such as contact time, pH, initial MB dye concentration, and temperature were studied in order to optimize the adsorption process.

The amount of MB dye adsorbed onto PNSM at equilibrium, q_e (mg/g) was computed as follows:

$$q_e = (C_o - C_e) \times \frac{V}{m} \quad (1)$$

where V is the volume of MB dye solution in liter, C_o and C_e are the initial and final concentrations of MB dye in solution, respectively, m is the weight (g) of PNSM.

For binary component system, 0.4 g of PNSM was added into 40 mL of 50 mg/L MB dye and with varying concentrations (1, 5 mg/L) of amaranth dye solutions in the conical flask. The solution was shaken at 100 rpm for 6 h to achieve equilibrium. PNSM was filtered off and the concentration of MB dye was determined as described above.

The adsorption kinetics experiment was carried out by agitating 200 mL aqueous solutions of MB dye of various concentrations with 2.0 g of PNSM at optimum pH. Fifty microliters of the samples was drawn out at various time intervals and the concentration of MB was determined. The experiment was continued until equilibrium was reached (when no further decrease in the MB dye concentration was measured). The effect of amaranth dye on the adsorption kinetics of MB dye was also testified. For this study, 2.0 g PNSM was shaken with 200 mL in a binary dye system containing 50 mg/L MB and 1–5 mg/L amaranth dyes at optimum pH. Adsorption isotherm studies were conducted at various temperatures (298–328 K).

2.5. Desorption studies

Several acids (HCl; H_2SO_4; citric acid; acetic acid; oxalic acid; H_3PO_4, and boric acid) of 0.1 M concentrations and solvents (acetone (Ac); ethanol (Et); and methanol (Mt)) were used as eluents for the desorption studies. The PNSM (0.2 g) was initially saturated with 40 mL MB solution of an initial concentration of 50 mg/L on a shaker at 100 rpm for 3 h. At equilibration, PNSM was filtered and washed several times with deionized water to remove MB traces. Then, PNSM was treated with 40 mL of aforementioned eluents. The flask was again shaken in a shaker at 100 rpm (to desorb MB) for 3 h and concentration of MB eluted was determined.

3. Results and discussion

The adsorption of MB and amaranth on PNSM was studied in single and binary systems. Preliminary studies in the single system at C_o—50 mg/L showed 20.27 and 1.03 mg/g MB and amaranth adsorption, respectively. The adsorption of MB in binary system (C_o of MB—50 mg/L and C_o of amaranth 5 mg/L) was 123.90 mg/g. In the binary system, amaranth dye favored the adsorption of MB onto PNSM. Due to the smaller hydrated radii of amaranth dye in comparison to MB, it adhered first onto the surface of PNSM. The amaranth dye is an anionic dye which made the surface of PNSM more negative, resulting in the higher adsorption of cationic MB dye onto the surface of PNSM.

3.1. Characterization of PNS biomass

Fig. 1(a) illustrates the FT-IR spectra of raw (PNS), modified (PNSM), and PNSM after MB adsorption (PNSM + MB). Bands at 3,363, 2,927, and 2,900 cm^{-1} were due to stretching of OH and C–H bonds [29]. Bands between 1,615 and 1,415 cm^{-1} were due to stretching of C=C aromatic rings. PNS biomass is a lignocellulosic material; the presence of cellulose in PNS was confirmed by a very weak band due to C–OH stretching of alcoholic and carboxylic acids at 1,034 cm^{-1}. After alkaline treatment, sharpening of bands at 3,359, 2,925, 2,900, and 1,035 cm^{-1} was observed. The sharpening of band at 1,034 cm^{-1} might be due to rupturing of lignin structure, making carbohydrates in the hetero-matrix, more accessible to binding adsorbate, and decreasing both the degree of polymerization and cellulose crystallinity [30]. After MB adsorption, the intensity of these bands reduced confirming active involvement of phenolic and carboxylic groups in the adsorption process of MB. The decrease in the crystallinity of the PNSM biomass after alkaline treatment was also confirmed by X-ray diffraction (XRD) results as peak intensity of PNSM was lower than PNS (Fig. 1(b)). The acid–base titration studies revealed a higher concentration of acidic sites

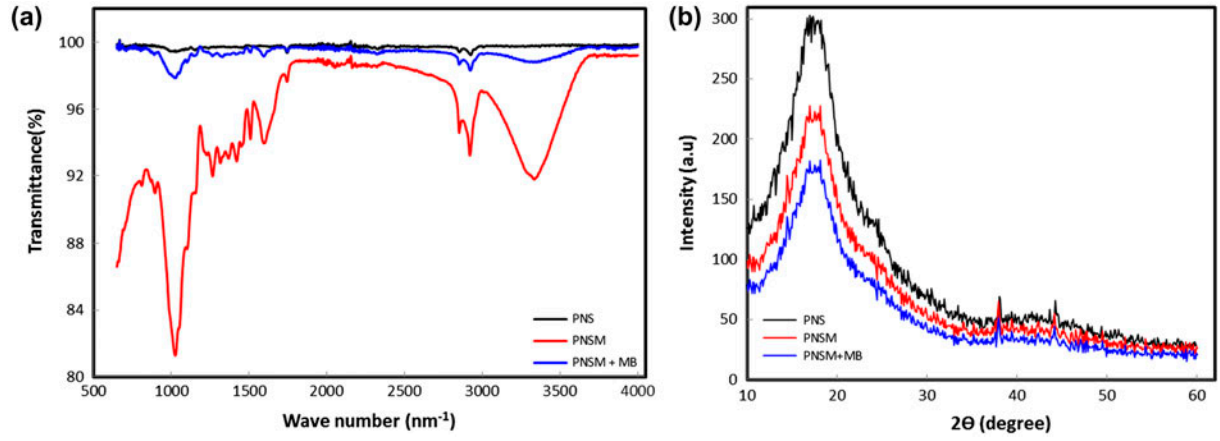

Fig. 1. FT-IR (a) and XRD (b) spectra of PNS biomass.

(3.22 meq/g) while, the concentration of basic sites was 0.22 meq/g. The Brunauer, Emmett and Teller (BET) results showed an extremely high surface area for PNS biomass (Table 1) which was reduced after alkaline treatment and MB adsorption on PNS which might be due to the introduction of functionalities and adherence of MB ions on the adsorbent surface blocked the pores of PNS. The SEM images of PNS showed a rough adsorbent surface with some irregular structures (Fig. 2(a)). After alkaline treatment, PNSM surface showed disappearance of those irregularities but fine pores dispersed over the surface (Fig. 2(b)). After MB adsorption, PNSM surface was totally occupied (Fig. 2(c)).

3.2. Effect of pH

Fig. 3(a) illustrates the effect of solution pH on MB adsorption on PNSM biomass. Under highly acidic conditions (i.e. pH_i 1.58–2.55), the surface of PNSM was highly protonated. The electrostatic and the adsorption capacity increased from 17.76 to 18.66 mg/g. A two-fold increase in the adsorption capacity was observed between pH_i 2.55 and 5.9. Maximum MB adsorption (39.73 mg/g) was observed at pH_i 5.9 which might be due to the proton reduction in aqueous medium. The surface charge of PNSM was determined by the solid addition method [27]. As seen in Fig. 3(b) the observed point of zero charge (pH_{PZC}) of PNSM was 6.35, which was nearer to pH_i at which maximum MB adsorption was observed. A further increase in pH_i from 5.9 to 9.87 showed no appreciable change in MB adsorption. Therefore, pH_i 6 was optimized for adsorption studies. At equilibrium, for initial pH range (pH_i) 1.58–5.9, the observed final aqueous phase pH (pH_f) was higher than the initial pH while, the pH_f was lower than the pH_i for pH_i 7.98–9.87 range, indicating buffering effect of PNSM in acid and alkaline mediums [31].

3.3. Effect of contact time and adsorption kinetics

Contact time studies were carried out in single and binary (with amaranth) systems. The initial concentration (C_o) range for MB adsorption in the single system on PNSM was 25–200 mg/L while, in the binary system C_o for MB was 50 mg/L (C_o for amaranth was 1 and 5 mg/L). In the single system, the equilibration time for MB C_o ranging 25–200 mg/L was 120 min, showing no effect of concentration on equilibration time. However, the adsorption capacity for the aforementioned concentration range increased from 8.91 to 78.82 mg/g (Fig. 4(a)). In the binary system, the concentration of amaranth affects equilibration time, reducing it to 90 min. The adsorption capacity in the binary system with C_o for MB—50 mg/L and C_o for amaranth 1 and 5 mg/L increased to 128.29 and

Table 1
BET surface area analysis

Sample	BET surface area (m^2/g)	Pore volume (cc/g)	Pore radius (nm)
Pine nut shells before modification (PNS)	266	0.060	45.36
Pine nut shells after modification (PNSM, before adsorption)	176	0.029	19.83
Pine nut shells after modification (PNSM, after MB adsorption)	110.9	0.014	11.78

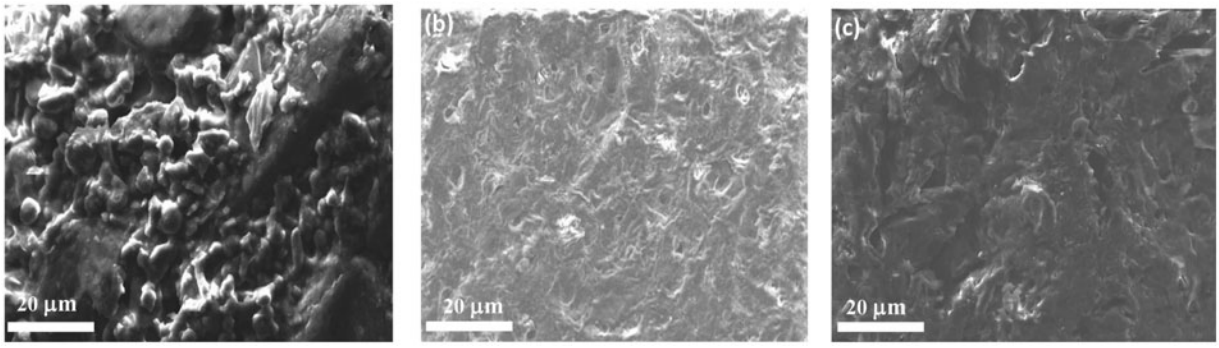

Fig. 2. SEM images of PNS (a), modified (PNSM) (b), and PNSM after MB adsorption (c).

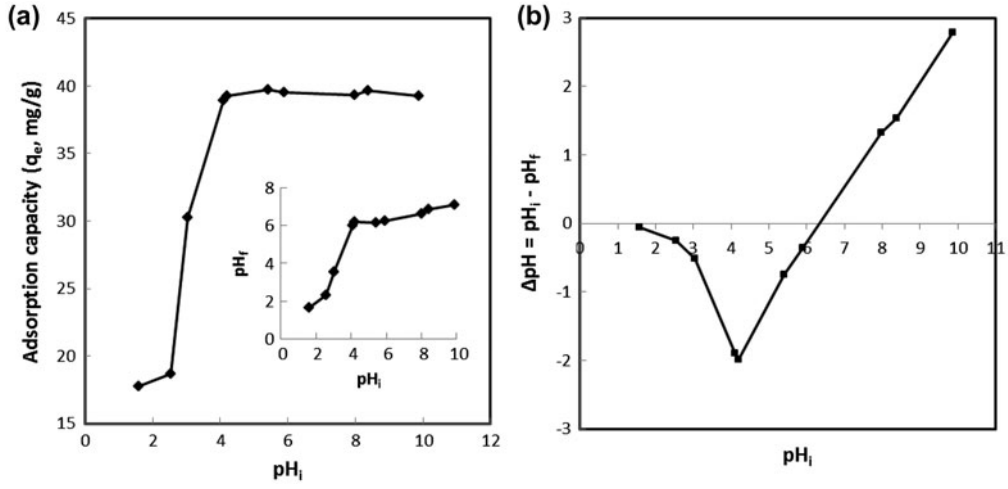

Fig. 3. Effect of pH on MB adsorption on pine nut shells (a) and point of zero charge (pH_{PZC}) plot (b).

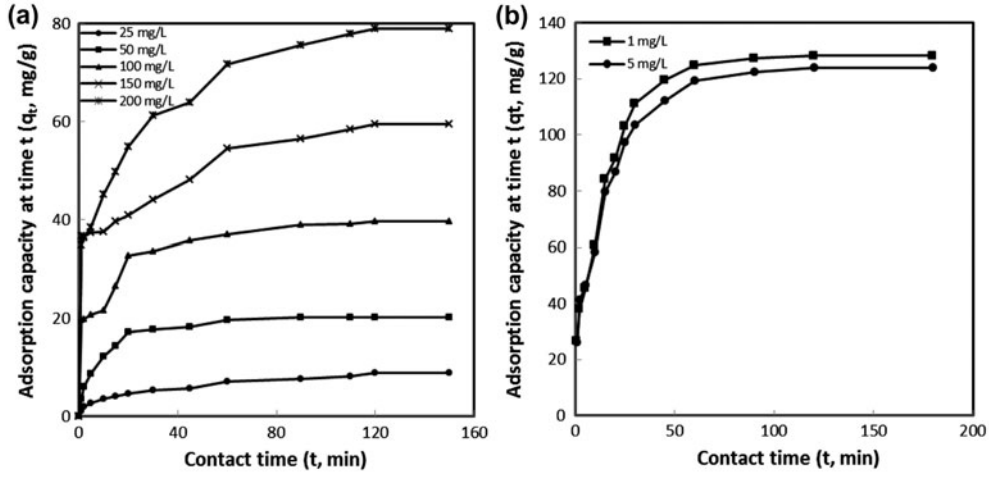

Fig. 4. Effect of contact time on MB adsorption at various concentrations in single system (a) and in binary system (at various amaranth concentrations) (b).

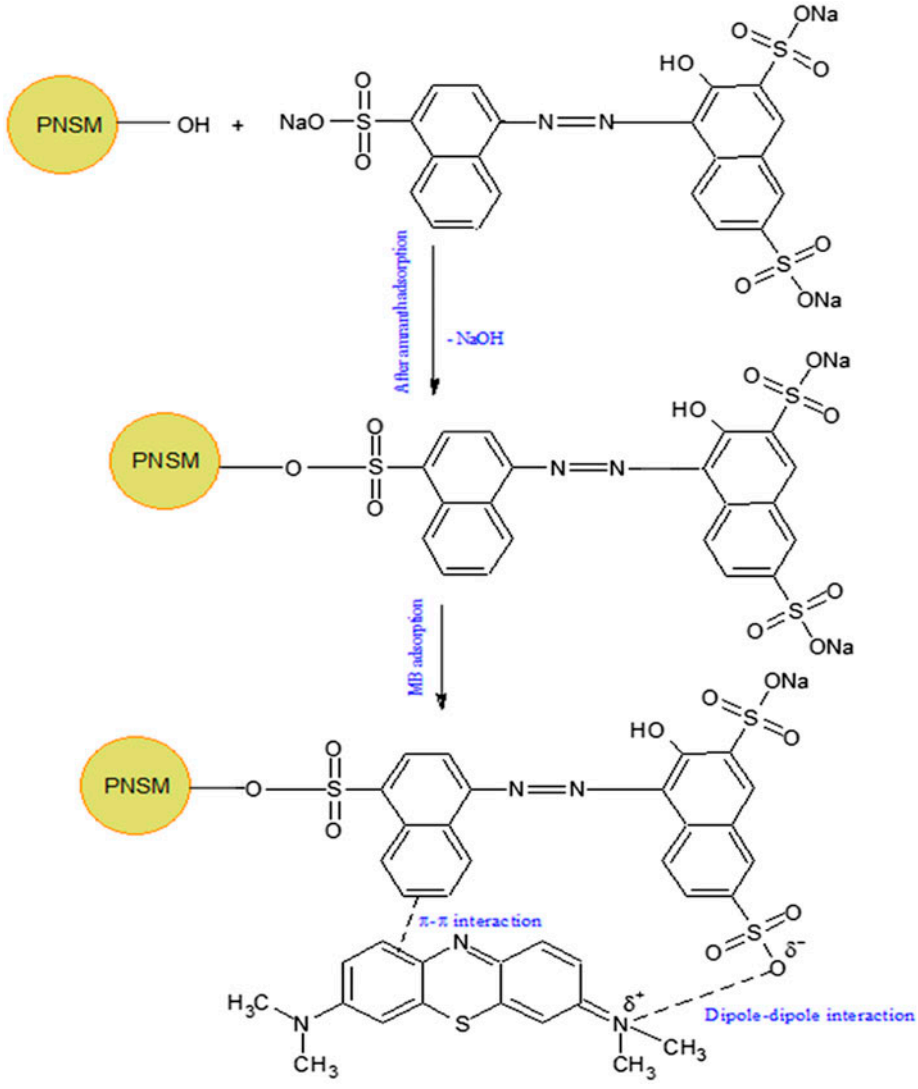

Fig. 5. Mechanism for the adsorption of MB onto PNSM.

123.83 mg/g, respectively (Fig. 4(b)). Compared to the single system, a six-fold increase in MB adsorption in the binary system was observed at similar experimental conditions. This showed that amaranth was playing a significant role to enhance MB adsorption. The adsorption mechanism is shown in Fig. 5.

Pseudo-first-order [32] and pseudo-second-order [33] kinetic models were applied which are given as:

$$\log(q_e - q_t) = \log q_e - \frac{k_1}{2.303} \times t \quad (2)$$

$$\frac{t}{q_t} = \frac{1}{k_2 q_e^2} + \frac{t}{q_e} \quad (3)$$

where q_e and q_t are the adsorption capacities at equilibrium and at time t, k_1, and k_2 are the pseudo-first-order and pseudo-second-order rate constants. The slopes and intercepts of the plots $\log(q_e - q_t)$ vs. t and t/q_t vs. t denote the rate constants and adsorption capacities, respectively.

The parameters as obtained from linearized plots (Fig. 6(a–d)) are given in Tables 2a and 2b. For both single and binary systems, the experimental adsorption capacity ($q_{e,exp}$) values at various MB concentrations were much closer to the calculated adsorption capacity ($q_{e,cal}$) values for pseudo-second-order model. These results were further confirmed by higher regression coefficient (R^2) values for pseudo-second-order model confirming better applicability of this model to adsorption data. From aforementioned results, it could be inferred that the MB adsorption onto PNSM was chemical in nature. In general, the adsorption process

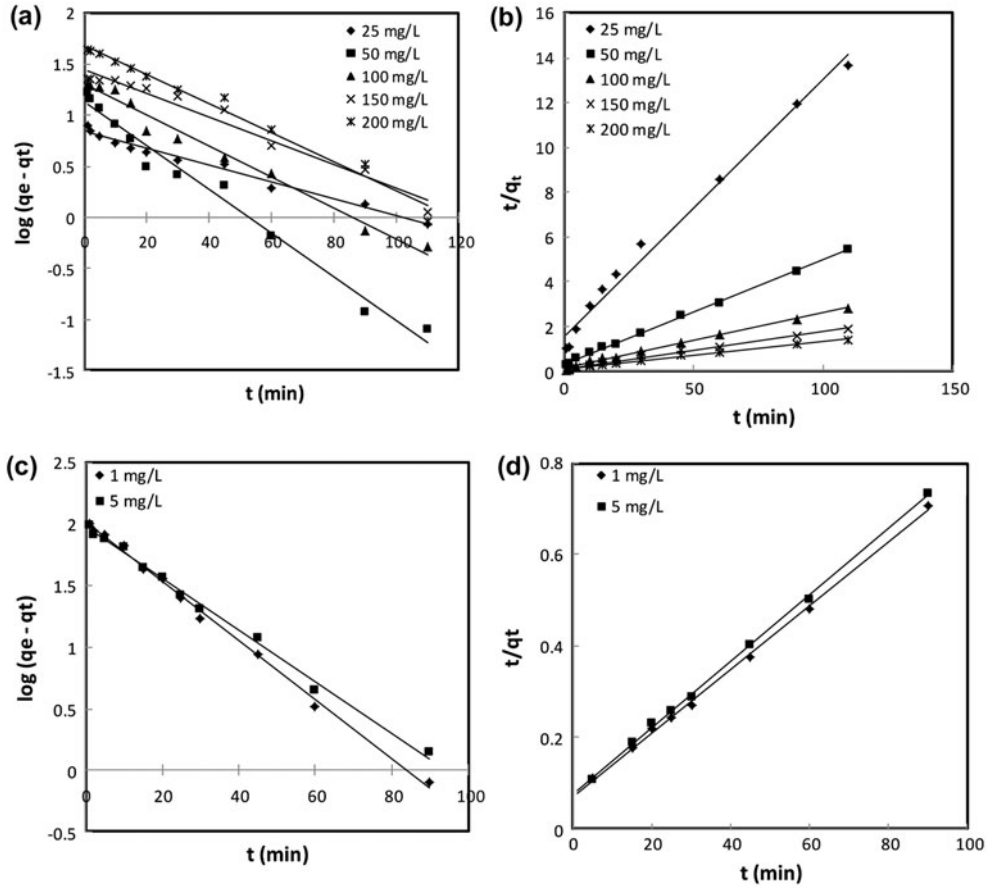

Fig. 6. Pseudo-first-order (a), pseudo-second-order (b) plots for the adsorption of MB in single system on PNSM at various concentrations; pseudo-first-order (c), and pseudo-second-order (d) plots for the adsorption of MB (C_o—50 mg/L) in binary system (in presence of amaranth at various concentrations) on PNSM.

Table 2a
Kinetic studies parameters for MB adsorption at various initial concentrations in single system on PNSM.

		Pseudo-first-order			Pseudo-second-order		
C_o (mg/L)	$q_{e,exp}$ (mg/g)	$q_{e,cal}$ (mg/g)	k_1 (1/min)	R^2	$q_{e,cal}$ (mg/g)	k_2 (g/mg-min)	R^2
25	8.91	6.896	0.0189	0.9813	8.72	0.0085	0.9877
50	20.27	13.561	0.0493	0.9812	21.41	0.0073	0.9991
100	39.68	20.267	0.0493	0.9812	40.65	0.0048	0.9962
150	59.53	28.314	0.0269	0.9689	59.52	0.0030	0.9908
200	78.92	48.607	0.0329	0.9790	80.64	0.0019	0.9924

Table 2b
Effect of amaranth concentration on kinetic studies parameters for MB adsorption (C_o—50 mg/L) on PNSM in binary mixture

Concentration of amaranth (mg/L)	$q_{e,exp}$ (mg/g)	Pseudo-first-order			Pseudo-second-order		
		$q_{e,cal}$ (mg/g)	k_1 (1/min)	R^2	$q_{e,cal}$ (mg/g)	k_2 (g/mg min)	R^2
1	128.28	104.09	0.0553	0.9967	142.86	0.00069	0.9985
5	123.90	95.21	0.0481	0.9951	136.99	0.00070	0.9991

is supposed to occur on the surface sites on the adsorbent where exchange and sharing of electrons via valance forces occurred. The process continues until the functional sites on the surface are fully saturated. In the single system, as the C_o of MB increases from 25 to 200 mg/L, the pseudo-second-order rate constant (k_2) decreases (Table 2a) which may be due to the decrease in the adsorption rate with increase in initial MB concentration.

Intra-particle diffusion model was given by Weber and Morris [34] as:

$$q_t = k_i\sqrt{t} + I \tag{4}$$

where k_i is the intra-particle diffusion constant and I represents the value of the thickness of the boundary layer. The slope and intercept of plot q_t vs. $\sqrt{t}$ gives intra-particle diffusion rate constant and boundary layer thickness values.

The slowest step during the adsorption process is the rate-determining step. Generally, the initial part of the adsorption is rapid due to external diffusion while the latter part (i.e. intra-particle mass transfer) is slow, will be a rate-determining step. Thus, intra-particle diffusion is one of the factors that affects the rate of attainment for the adsorption to reach equilibrium state [35]. Fig. 7(a) and (b) illustrates Weber and Morris plots for the adsorption of MB in single and binary systems on PNSM. The plots showed multi-linearity with deviation from origin, confirming that intra-particle diffusion is not the only mechanism involving in the adsorption process [36]. Initially, due to film diffusion the adsorption rate was very high. As MB concentration on PNSM external surface increases, there is an immediate occupation of active sites of the adsorbent. As reaction continues, the adsorption was controlled by intra-particle diffusion. Since the rate of adsorption slows down, this region is also known as the rate-determining step. Finally, the plateau segment was reached, indicating attainment of the equilibrium state. At this point, maximum MB adsorption on PNSM occurred. The equilibrium stage at the end was due to the decrease in the number of active sites available for the adsorption as well as low bulk concentration of MB. The values of k_i and I are given in Tables 3a and 3b. For the single system, the intra-particle diffusion rate, k_i increases with the increase in initial MB concentration while for the binary system, a very little decrease in k_i values with the increase in initial amaranth concentration was observed. The increase in MB adsorption in the single system was due to the higher number of MB molecules present in the solution which largely occupy the active sites on PNSM surface. In the binary system, the increase in amaranth concentration leads to a competition to occupy surface active sites.

Table 3a
Intra-particle diffusion parameters for MB adsorption in single system at various initial concentrations on PNSM

C_o (mg/L)	K_i (mg/g min$^{1/2}$)	I	R^2
25	0.6852	1.1259	0.9761
50	1.3627	6.9274	0.7836
100	2.0251	18.812	0.8775
150	2.4472	31.970	0.9620
200	4.3389	32.612	0.9574

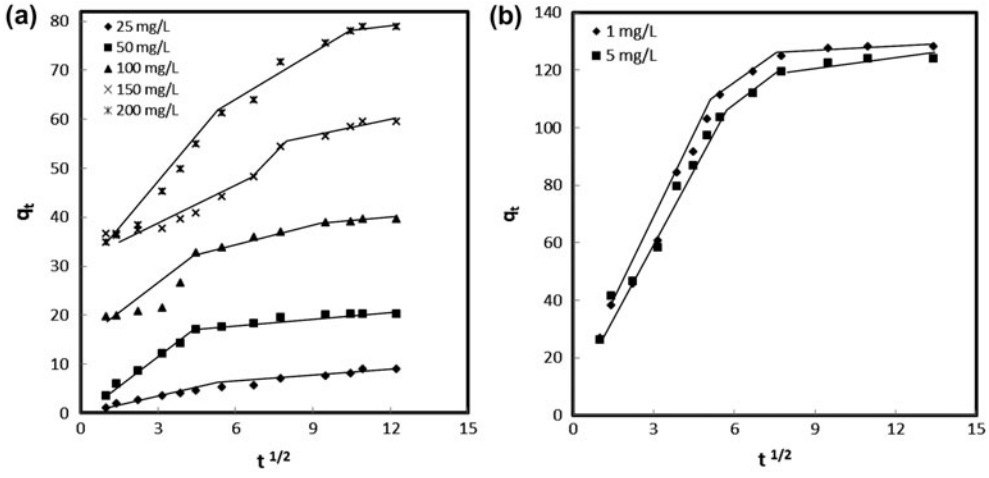

Fig. 7. Weber and Morris plots for the adsorption of MB at various concentrations in single system on PNSM (a) and in binary system (in presence of amaranth at various concentrations) on PNSM (b).

Table 3b
Effect of amaranth concentration on intra-particle diffusion parameters for MB adsorption (C_o—50 mg/L) in binary system on PNSM

C_o (mg/L)	K_i (mg/g min$^{1/2}$)	I	R^2
1	8.6569	41.665	0.7735
5	8.1976	40.554	0.8014

An increase in I values with an increase in initial MB concentration, attributes to a greater effect of the boundary layer at a higher MB concentration in the single system while, in the binary system, a slight decrease in I values was observed. Thus, the thicker the boundary layer surrounding the adsorbent eventually the higher the uptake of MB [37].

3.4. Effect of concentration and adsorption isotherms

The effect of MB concentration as a function of reaction temperature (298–328 K) was studied. Initially, the adsorption of MB on PNSM was rapid, and then slows down attaining equilibrium point. The adsorption increases with an increase in the initial MB concentration as it is providing a driving force to overcome mass transfer resistance between solid/solution interfaces. Though, the adsorption increases with an increase in the reaction temperature, no profound effect of the reaction temperature on the MB adsorption was observed (Fig. 8).

The efficacy of adsorption process is determined by adsorption isotherms. In this study, the adsorption data

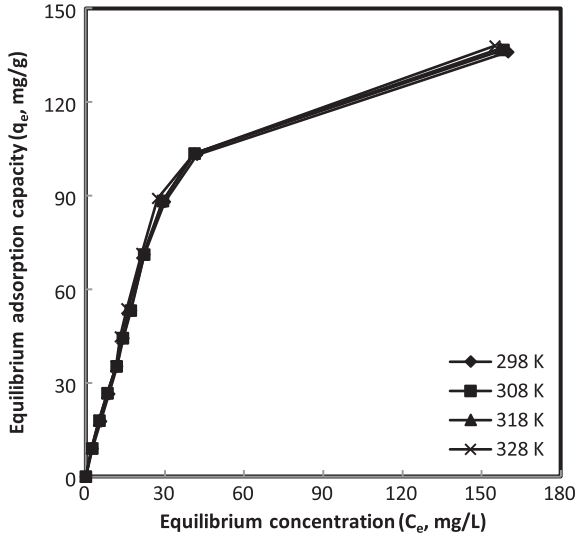

Fig. 8. Effect of concentration on MB adsorption onto PNSM at various temperatures.

were modeled by two parameters Langmuir and Freundlich isotherms. The linearized forms of Langmuir [38] and Freundlich [39] models are given as:

$$\frac{C_e}{q_e} = \frac{1}{bq_m} + \frac{1}{q_m} \times C_e \quad (5)$$

$$\log q_e = \log K_f + \frac{1}{n} \log C_e \quad (6)$$

where q_m is the Langmuir constant for maximum solid phase loading on adsorbent, b is an energy constant related to the heat of adsorption, K_f is a Freundlich constant related to bond energy and n represents adsorption deviation from linearity. The slopes and intercepts of the plots C_e/q_e vs. C_e and log q_e vs. log C_e gives values of q_m, K_f, and n.

The essential feature of the Langmuir model can be expressed by dimensionless constant separation faction (R_L). It is given as:

$$R_L = \frac{1}{1 + bC_o} \quad (7)$$

The value of R_L reflects the nature of adsorption. If $R_L > 1$ (unfavorable), $0 < R_L < 1$ (favorable), $R_L = 1$ (linear), $R_L = 0$ (irreversible).

Fig. 9(a) and (b) illustrates linearized Langmuir and Freundlich plots. The parameters obtained by linearized plots are given in Table 4. Results showed higher regression coefficient (R^2) values for the Freundlich model at various temperatures confirming better fitting of the model to experimental data. Table 5 presents a summary of previously applicable models on the MB adsorption on various adsorbents. The values of R_L in between 0 and 1 showed a favorable adsorption process.

3.5. Adsorption thermodynamics

The thermodynamic studies for the adsorption of MB at various concentrations on PNSM were carried out for temperature range 298–328 K. The adsorption capacity at various concentrations increases with an increase in the temperature confirming chemisorption process. Thermodynamic parameters such as Gibb's free energy change (ΔG°), standard enthalpy change (ΔH°), and standard entropy change (ΔS°) were also determined.

The ΔG° values are calculated as:

$$\Delta G^\circ = \Delta H^\circ - T\Delta S^\circ \quad (8)$$

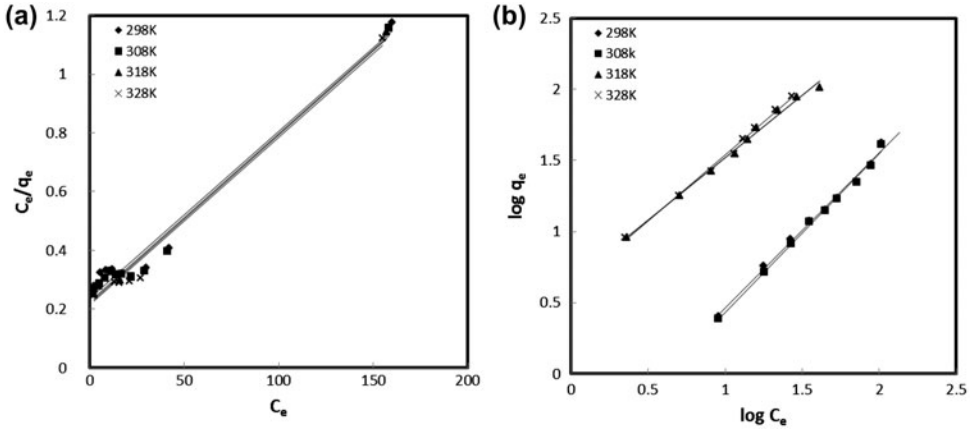

Fig. 9. Langmuir (a) and Freundlich (b) isotherm plots for the adsorption of MB on PNSM.

Table 4
Isotherm studies parameters for the adsorption of MB on PNSM

	Langmuir isotherm				Freundlich isotherm		
Temp. (K)	q_m (mg/g)	b (L/mg)	R^2	R_L	K_f (mg/g) $(L/mg)^{1/n}$	n	R^2
298	175.43	0.0241	0.9697	0.0766	0.2396	0.9205	0.9931
308	177.42	0.0252	0.9767	0.0735	0.2089	0.8981	0.9955
318	179.45	0.0259	0.9786	0.0716	7.5680	1.1376	0.9945
328	182.08	0.0266	0.9763	0.0699	8.4411	1.0794	0.9950

Table 5
Summary of MB adsorption results on various adsorbents

	Models applicable			
Adsorbent	Isotherm	Kinetics	Thermodynamics	Refs.
Garlic peel	Freundlich	Pseudo-second-order	Endothermic	[40]
Coir pith carbon	Langmuir and Temkin	Pseudo-second-order	Endothermic	[41]
Sugar extracted spent rice biomass	Langmuir	Pseudo-second-order	Endothermic	[42]
Eucalyptus sheathiana bark	Langmuir	Pseudo-second-order	Endothermic	[43]
PNSM	Freundlich	Pseudo-second-order	Endothermic	Present study

The values of K_c are given as:

$$K_c = \frac{C_{Ae}}{C_e} \tag{9}$$

where C_{Ae} (mg/L) and C_e (mg/L) are the equilibrium concentrations of adsorbate on solid and in solution phase, respectively.

Von't Hoff equation was used to calculate the value of ΔH° and ΔS° given as:

$$\ln K_c = \frac{\Delta S^\circ}{R} - \frac{\Delta H^\circ}{R} \times \frac{1}{T} \tag{10}$$

The plot ln K_c vs. $1/T$ (Fig. 10) was used to evaluate ΔH° and ΔS° values. Table 6 presents the thermodynamic studies' data for the adsorption of MB at various concentrations on PNSM. The negative values of ΔG° indicate that spontaneous adsorption process and spontaneity increases with increase in the temperature. The positive values of

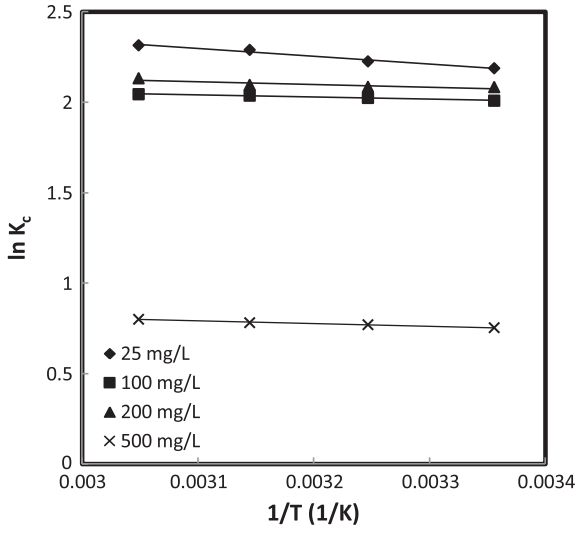

Fig. 10. Van't Hoff plot for the adsorption of MB on PNSM.

ΔS° indicated the disorderliness at the adsorbent surface during the adsorption process. Moreover, the positive value of ΔH° proved that the adsorption of MB on PNSM was an endothermic process.

3.6. Effect of counter ions

The industrial, municipal, and domestic effluents' matrix along with dyes also contains many anions and cations. Therefore, in this study, we have tested the potentiality of PNSM for the removal of MB (C_o—50 mg/L) in the presence of the counter ions. A control experiment was also carried out to compare the values. The adsorption capacity of MB during the control experiment was 20.27 mg/g while, the adsorption capacity of MB in the presence of K^+ ions was the highest and in the presence of Ca^{2+} ions was the lowest (Table 7). The MB adsorption capacity in the presence of monovalent sodium (Na^+) and potassium (K^+) ions for concentration range 5–25 mg/L varied between 17.730–16.608 and 18.904–16.977 mg/g, respectively, while in the presence of divalent magnesium (Mg^{2+}) and calcium (Ca^{2+}) ions for concentration range 5–25 mg/L the MB adsorption capacity varied between 15.307–14.890 and 17.157–16.095 mg/g, respectively (Table 7). Here, it is noteworthy that hydrated radii and ionic charge of the counter ions played a critical role in hindering MB adsorption. The hydrated radii of Mg^{2+} (1.08) was the highest, therefore causing maximum hindrance in MB adsorption followed Ca^{2+} (0.96) > Na^+ (0.79) > K^+ (0.53).

3.7. Desorption studies

Fig. 11 illustrates MB recovery plot. The recovery of MB with acids was maximum while, the recovery with solvents such as EtOH, MeOH, and Ac was 27.48, 7.47, and 6.75%, respectively. Among the acids, 92.54% (maximum) MB was eluted by 0.1 M OA followed by 0.1 M PA (84.86%), 0.1 M SA (83.35%), 0.1 M CA (78.07%), 0.1 M HA (76.01%), and 0.1 M AA (35.32%), and 0.1 M BA (9.35%). Similar results for MB desorption were reported elsewhere [30].

Table 6
Thermodynamic studies parameters for the adsorption of MB on PNSM

MB initial concentration (C_o, mg/L)	Temp. (K)	k_c	ΔG° (−) (kJ/mol)	ΔH° (kJ/mol)	ΔS° (J/mol K)
25	298	8.917	56.29	36.09	0.31
	308	9.263	59.39		
	318	9.869	62.49		
	328	10.121	65.59		
100	298	7.452	49.82	9.78	0.20
	308	7.567	51.82		
	318	7.664	53.84		
	328	7.724	55.82		
200	298	8.033	51.62	12.57	0.21
	308	8.045	53.39		
	318	8.132	55.41		
	328	8.435	58.15		
500	298	2.125	18.67	12.18	0.10
	308	2.160	19.72		
	318	2.185	20.66		
	328	2.226	21.81		

Table 7
Effect of counter ions on MB adsorption on PNSM

Counter ions	Concentration of counter ions (mg/L)	Adsorption capacity of MB (mg/g)
Na^+	5	17.730
	10	17.534
	15	17.215
	20	16.894
	25	16.608
K^+	5	18.904
	10	18.484
	15	17.667
	20	17.231
	25	16.977
Mg^{2+}	5	15.307
	10	15.292
	15	15.166
	20	15.067
	25	14.890
Ca^{2+}	5	17.157
	10	16.969
	15	16.702
	20	16.325
	25	16.095

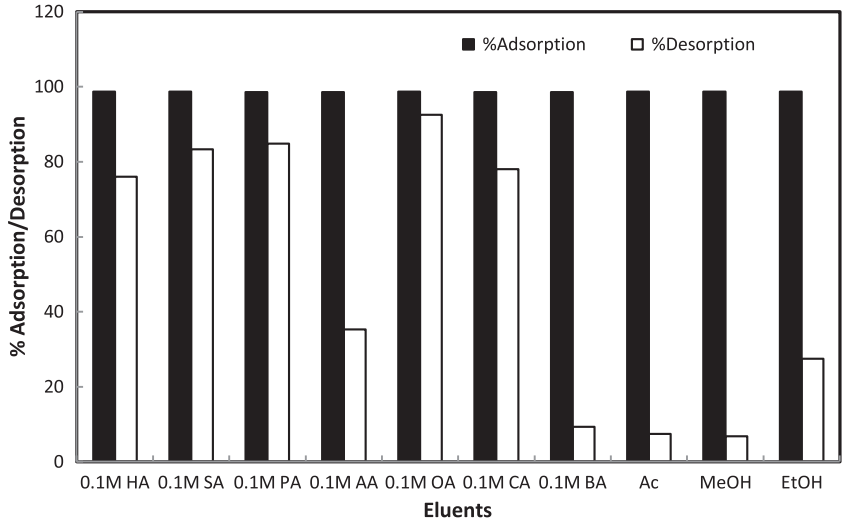

Fig. 11. Batch desorption studies of MB from PNSM.

4. Conclusions

In the present research, we have tested the fate of PNSM for the selective adsorption of MB from a binary mixture of dyes. It was observed that PNSM had a higher adsorption capacity for MB in comparison to amaranth dye. The adsorption of MB onto PNSM was also favored by the presence of amaranth dye. The anionic nature of amaranth dye might increase anion concentrations over the PNSM surface, resulting in a higher adsorption of cationic MB dye onto the surface of PNSM. The kinetics data were best fitted in the pseudo-second-order rate equation as evident from the values of regression coefficients (R^2). The adsorption isotherm studies showed that the Freundlich

model was better fitted. The positive value of ΔH° and ΔS° indicated endothermic adsorption process and MB adsorption caused the randomness in the system. Thus, it could be concluded that PNSM is an economically appealing and ecologically safe adsorbent for selective MB dye adsorption.

Acknowledgment

This project was supported by King Saud University, Deanship of Scientific Research, College of Science Research Center.

References

[1] M. Ghaedi, S. Hajati, F. Karimi, B. Barazesh, G. Ghezelbash, Equilibrium, kinetic and isotherm of some metal ion biosorption, J. Ind. Eng. Chem. 19 (2015) 987–992.
[2] T.K. Sen, S. Afroze, H.M. Ang, Equilibrium, kinetics and mechanism of removal of methylene blue from aqueous solution by adsorption onto pine cone biomass of *Pinus radiata*, Water Air Soil Pollut. 218 (2011) 499–515.
[3] F. Marahel, M.A. Khan, E. Marahela, I. Bayestia, I. Hosseini, Kinetics, thermodynamics, and isotherm studies for the adsorption of BR_2 dye onto avocado integument, Desalin. Water Treat. (2013), doi: 10.1080/19443994.2013.846240.
[4] S. Hajati, M. Ghaedi, F. Karimi, B. Barazesh, R. Sahraei, A. Daneshfar, Competitive adsorption of Direct Yellow 12 and Reactive Orange 12 on ZnS: Mn nanoparticles loaded on activated carbon as novel adsorbent, J. Ind. Eng. Chem. 20 (2014) 564–571.
[5] M. Naushad, M.A. Khan, Z.A. ALOthman, M.R. Khan, Adsorptive removal of nitrate from synthetic and commercially available bottled water samples using De-Acidite FF-IP resin, J. Ind. Eng. Chem. 20 (2014) 3400–3407.
[6] H. Javadian, M.T. Angaji, M. Naushad, Synthesis and characterization of polyaniline/γ-alumina nanocomposite: A comparative study for the adsorption of three different anionic dyes, J. Ind. Eng. Chem. 20 (2014) 3890–3900.
[7] M.A. Khan, M. Ngabura, T.S.Y. Choong, H. Masood, L.A. Chuah, Biosorption and desorption of nickel on oil cake: Batch and column studies, Bioresour. Technol. 103 (2012) 35–42.
[8] G. Sharma, M. Naushad, D. Pathania, A. Mittal, G.E. El-desoky, Modification of *Hibiscus cannabinus* fiber by graft copolymerization: Application for dye removal, Desalin. Water Treat. 54 (2015) 3114–3121.
[9] M.A. Khan, Z.A. ALOthman, M. Naushad, M.R. Khan, M. Luqman, Adsorption of methylene blue on strongly basic anion exchange resin (Zerolit DMF): Kinetic, isotherm and thermodynamic studies, Desalin. Water Treat. 53 (2015) 515–523.
[10] A. Kumar, G. Sharma, M. Naushad, S. Kalia, P. Singh, Polyacrylamide/Ni 0.02 Zn 0.98 O nanocomposite with high solar light photocatalytic activity and efficient adsorption capacity for toxic dye removal, J. Ind. Eng. Chem. Res. 53 (2014) 15549–15560.
[11] C.-H. Weng, Y.-T. Lin, T.-W. Tzeng, Removal of methylene blue from aqueous solution by adsorption onto pineapple leaf powder, J. Hazard. Mater. 170 (2009) 417–424.
[12] V.K. Garg, M. Amita, R. Kumar, R. Gupta, Basic dye (methylene blue) removal from simulated wastewater by adsorption using Indian Rosewood sawdust: A timber industry waste, Dyes Pigm. 63 (2004) 243–250.
[13] J. Pavel, H. Buchtova, M. Ryznarova, Sorption of dyes from aqueous solutions onto flyash, Water Res. 37 (2003) 4938–4944.
[14] T. Robinson, B. Chandra, P. Nigam, Removal of dyes from a synthetic textile dye effluent by biosorption on apple pomace and wheat straw, Water Res. 36 (2002) 2824–2830.
[15] Y. Fu, T. Viraraghavan, Removal of congo red from an aqueous solution by fungus *Aspergillus niger*, Adv. Environ. Res. 7 (2002) 239–247.
[16] M. Arami, N.Y. Limaee, N.M. Mahmoodi, N.S. Tabrizi, Removal of dyes from colored textile wastewater by orange peel adsorbent: Equilibrium and kinetic studies, J. Colloid Interf. Sci. 288 (2005) 371–376.
[17] M. Arami, N.Y. Limaee, N.M. Mahmoodi, N.S. Tabrizi, Equilibrium and kinetics studies for the adsorption of direct and acid dyes from aqueous solution by soy meal hull, J. Hazard. Mater. 135 (2006) 171–179.
[18] M. Turabik, Adsorption of basic dyes from single and binary component systems onto bentonite: Simultaneous analysis of Basic Red 46 and Basic Yellow 28 by first order derivative spectrophotometric analysis method, J. Hazard. Mater. 158(1) (2008) 52–64.
[19] Y. Fan, H.-J. Liu, Y. Zhang, Y. Chen, Adsorption of anionic MO or cationic MB from MO/MB mixture using polyacrylonitrile fiber hydrothermally treated with hyperbranched polyethylenimine, J. Hazard. Mater. 283 (2015) 321–328.
[20] M. Auta, B.H. Hameed, Optimized and functionalized paper sludge activated with potassium fluoride for single and binary adsorption of reactive dyes, J. Ind. Eng. Chem. 20(3) (2014) 830–840.
[21] S. Dawood, T.K. Sen, Removal of anionic dye Congo red from aqueous solution by raw pine and acid-treated pine cone powder as adsorbent: Equilibrium, thermodynamic, kinetics, mechanism and process design, Water Res. 46 (2012) 1933–1946.
[22] P. Senthil Kumar, S. Ramalingam, C. Senthamarai, M. Niranjanaa, P. Vijayalakshmi, S. Sivanesan, Adsorption of dye from aqueous solution by cashew nut shell: Studies on equilibrium isotherm, kinetics and thermodynamics of interactions, Desalination 261 (2010) 52–60.
[23] G. Sreelatha, V. Ageetha, J. Parmar, P. Padmaja, Equilibrium and kinetic studies on reactive dye adsorption using palm shell powder (an agrowaste) and chitosan, J. Chem. Eng. Data 56 (2011) 35–42.
[24] N.A. Oladoja, C.O. Aboluwoye, Y.B. Oladimeji, A.O. Ashogbon, I.O. Otemuyiwa, Studies on castor seed shell as a sorbent in basic dye contaminated wastewater remediation, Desalination 227 (2008) 190–203.
[25] G. McKay, K.K.H. Choy, J.F. Porter, Langmuir isotherm models applied to the multicomponent sorption of acid dyes from effluent onto activated carbon, J. Chem. Eng. Data 45 (2000) 575–584.

[26] B. Noroozi, G.A. Sorial, H. Bahrami, M. Arami, Adsorption of binary mixtures of cationic dyes, Dyes Pigm. 76 (2008) 784–791.
[27] M.A. Khan, S.-W. Kim, R.A.K. Rao, R.A.I. Abou-Shanab, A. Bhatnagar, H. Song, B.-H. Jeon, Adsorption studies of dichloromethane on some commercially available GACs: Effect of kinetics, thermodynamics and competitive ions, J. Hazard. Mater. 178 (2010) 963–972.
[28] H.P. Boehm, Some aspects of the surface chemistry of carbon blacks and other carbons, Carbon 32 (1994) 759–769.
[29] D.L. Pavia, G.M. Lampman, G.S. Kriz, Introduction to Spectroscopy, second ed., Saunders Golden Sunburst Series, New York, NY, 1996.
[30] M.R. Khan, M.A. Khan, Z.A. Alothman, I.H. Alsohaimi, M. Naushad, N.H. Al-Shaalan, Quantitative determination of methylene blue in environmental samples by solid-phase extraction and ultra-performance liquid chromatography-tandem mass spectrometry: A green approach, RSC Adv. 4 (2014) 34037–34044.
[31] M.A. Khan, Z.A. AlOthman, M. Kumar, M.S. Ola, M.R. Siddique, Biosorption potential assessment of modified pistachio shell waste for methylene blue: Thermodynamics and kinetics study, Desalin. Water Treat. (2014), doi: 10.1080/19443994.2014.934728.
[32] S. Lagergren, About the theory of so-called adsorption of soluble substances, K. Sven. Vetenskapsakad, Handl. 24 (1898) 1–39.
[33] Y.S. Ho, G. McKay, The kinetics of sorption of divalent metal ions onto sphagnum moss peat, Water Res. 34 (2000) 735–742.
[34] W.J. Weber Jr., J.C. Morris, Kinetics of adsorption on carbon from solution, J. Sanitary Eng. Div. Am. Soc. Chem. Eng. 89 (1963) 31–59.
[35] W. Cheah, S. Hosseini, M.A. Khan, T.G. Chuah, T.S.Y. Choong, Acid modified carbon coated monolith for methyl orange adsorption, Chem. Eng. 215–216 (2013) 747–754.
[36] W.H. Cheung, Y.S. Szeto, G. McKay, Intraparticle diffusion processes during acid dye adsorption onto chitosan, Bioresour. Technol. 98 (2007) 2897–2904.
[37] N. Kannan, M.M. Sundaram, Kinetics and mechanism of removal of methylene blue by adsorption on various carbons-a comparative study, Dyes Pigm. 51 (2001) 25–40.
[38] I. Langmuir, The adsorption of gases on plane surface of glass, mica and platinum, J. Am. Chem. Soc. 40 (1916) 1361–1403.
[39] H.M.F. Freundlich, Over the adsorption in solution, J. Phys. Chem. 57 (1906) 385–470.
[40] B.H. Hameed, A.A. Ahmad, Batch adsorption of methylene blue from aqueous solution by garlic peel, an agricultural waste biomass, J. Hazard. Mater. 164 (2009) 870–875.
[41] D. Kavitha, C. Namasivayam, Experimental and kinetic studies on methylene blue adsorption by coir pith carbon, Bioresour. Technol. 98 (2007) 14–21.
[42] M.S. Rehman, I. Kim, J.-I. Han, Adsorption of methylene blue dye from aqueous solution by sugar extracted spent rice biomass, Carbohydr. Polym. 90 (2012) 1314–1322.
[43] S. Afroze, T.K. Sen, M. Ang, H. Nishiok, Adsorption of methylene blue dye from aqueous solution by novel biomas *Eucalyptus sheathiana* bark: Equilibrium, kinetics, thermodynamics and mechanism, Desalin. Water Treat. (2015), doi: 10.1080/19443994.2015.1004115.